Mon. Not. R. Astron. Soc. **000**, 1–?? (2015) Printed 9 March 2016 (MN LATEX style file v2.2)

Period-Luminosity relations derived from the OGLE-III First-overtone mode Cepheids in the Magellanic Clouds

Anupam Bhardwaj[1⋆], Chow-Choong Ngeow[2], Shashi M. Kanbur[3] and Harinder P. Singh[1]

1. Department of Physics & Astrophysics, University of Delhi, Delhi 110007, India
2. Graduate Institute of Astronomy, National Central University, Jhongli 32001, Taiwan
3. State University of New York, Oswego, NY 13126, USA

arXiv:1603.02582v1 [astro-ph.GA] 8 Mar 2016

Accepted 2016 March 8. Received 2016 March 8; in original form 2015 December 8

ABSTRACT

We present multi-band Period-Luminosity (PL) relations for first-overtone mode Cepheids in the Small Magellanic Cloud (SMC). We derive optical band PL relations and the Wesenheit function using VI mean magnitudes from the Optical Gravitational Lensing Experiment (OGLE-III) survey. We cross-match OGLE-III first-overtone mode Cepheids to the 2MASS and SAGE-SMC catalogs to derive PL relations at near-infrared (JHK_s) and mid-infrared (3.6 & 4.5μm) wavelengths. We test for possible non-linearities in these PL relations using robust statistical tests and find a significant break only in the optical-band PL relations at 2.5 days for first-overtone mode Cepheids. We do not find statistical evidence for a non-linearity in these PL relations at 1 day. The multi-band PL relations for fundamental-mode Cepheids in the SMC also exhibit a break at 2.5 days. We suggest that the period break around 2.5 days is related to sharp changes in the light curve parameters for SMC Cepheids. We also derive new optical and mid-infrared band PL relations for first-overtone mode Cepheids in the Large Magellanic Cloud (LMC). We compare multi-band PL relations for first-overtone mode Cepheids in the Magellanic Clouds and find a significant difference in the slope of the V-band PL relations but not for I-band PL relations. The slope of PL relations are found to be consistent in most of the infrared bands. A relative distance modulus of $\Delta\mu = 0.49 \pm 0.02$ mag between the two clouds is estimated using multi-band PL relations for the first-overtone mode Cepheids in the SMC and LMC.

Key words: stars: variables: Cepheids, (galaxies:) Magellanic Clouds.

1 INTRODUCTION

The Period-Luminosity (PL) relation for Cepheid variables is a vital tool in the cosmic distance ladder to obtain distances to the Local Group galaxies and determine an accurate and precise value of the Hubble constant (Riess et al. 2009, 2011) that is independent of the Cosmic Microwave Background (*Planck* collaboration, Ade et al. 2014). The PL relation or the Leavitt law was first introduced by Leavitt & Pickering (1912) for Cepheids in the Small Magellanic Cloud (SMC). Following this, many studies were published concerning PL relations at optical and near-infrared wavelengths for Cepheids in the SMC (for example, Welch & Madore 1984; Laney & Stobie 1986; Welch et al. 1987; Caldwell & Laney 1991; Laney & Stobie 1994, and references therein). At optical wavelengths, the second phase of the Optical Gravitational Lensing Experiment (OGLE-II) survey derived PL relations for Cepheid variables (Udalski et al. 1999a). Later, this catalog was used in many studies on PL and/or Period-Color (PC) relations (Udalski et al. 1999b; Sharpee et al. 2002; Storm et al. 2004; Sandage, Tammann & Reindl 2009). Similarly, the PL relations for $\sim$ 600 Cepheids in the SMC were derived by the EROS (Expérience de Recherche d'Objets Sombres) collaboration (Bauer et al. 1999). Further, Groenewegen (2000) used Cepheids in the Magellanic Clouds from OGLE-II and their counterparts in 2MASS and DENIS catalogs to derive infrared band PL relations.

In the past decade, a catalog of a large number of Cepheids in the SMC was released by the third phase

⋆ E-mail: anupam.bhardwajj@gmail.com

of OGLE survey (OGLE III, Soszyñski et al. 2010). The authors provided optical band PL and Period-Wesenheit (PW) relations for fundamental and first-overtone mode Cepheids but these relations did not take account of extinction corrections. At infrared wavelengths, Ngeow & Kanbur (2010) and Ngeow, Citro & Kanbur (2012) derived PL relations for Cepheids using *Spitzer* and *AKARI* archival data. Sandage, Tammann & Reindl (2009) derived fundamental mode PL and PC relations for Cepheids in the SMC and Tammann, Reindl & Sandage (2011) extended this work to first-overtone mode Cepheids and compared these relations with those of Cepheids in metal-poor Local Group galaxies. Further, Matsunaga, Feast & Soszyński (2011) used OGLE-III counterparts of SMC Cepheids in the IRSF observations to derive PL relations and Inno et al. (2013) used these random phase observations to derive PW relations. Recently, Subramanian & Subramaniam (2015) also derived the PL and PC relations for the OGLE-III Classical Cepheids and investigated the structure of the SMC.

Many studies in the literature concentrate on fundamental mode Cepheid PL relations for their application to the distance scale. Therefore, very few of these studies have derived PL relations for the first-overtone mode Cepheids in the Magellanic Clouds, specially at infrared wavelengths. Recently, Ngeow et al. (2015) derived multi-band PL relations for fundamental mode Cepheids in the SMC. They also used various test statistics to find evidence of a possible non-linearity at 10 days and provided evidence that the SMC PL relations are linear. However, they only concentrated on the Cepheid samples with $P > 2.5$ days. The reason is that the EROS collaboration found a break in the PL relation for Cepheids with periods shorter than 2 days (Bauer et al. 1999). This was later confirmed in many studies (for example, Tammann, Reindl & Sandage 2011; Subramanian & Subramaniam 2015) but at a slightly different period. Further, Bhardwaj et al. (2014) have shown that both fundamental and the first-overtone mode Cepheids in the SMC exhibit break at 2.5 days in PC and Amplitude-Color (A-C) relations at maximum and minimum light in optical bands. For these reasons, we extend previous work to study multi-band SMC PL relations for the first-overtone mode Cepheids and short period fundamental mode Cepheid PL relations to rigorously test for nonlinearity at various periods.

This paper is structured as follows. In Section 2, we discuss the optical, near-infrared and mid-infrared data for SMC Cepheid variables used in our analysis along with the extinction corrections. We derive multi-band PL relations for first-overtone mode Cepheids in the SMC in Section 3, and compare these with published results. We also test these relations for non-linearity at various periods. We compare breaks in the first-overtone mode PL relations with the short period break in fundamental mode SMC Cepheid PL relations (§4). We also compare the first-overtone multi-band PL relations for Cepheids in the two Magellanic clouds (§5). Finally, the results and important conclusions of this study are discussed in Section 6.

Table 1. Summary of the matched SAGE-SMC archival data for SMC FO mode Cepheids.

Band	epoch	$N_{\rm match}$	$<\Delta>^a$	σ^b	^{c}(in %)
3.6μm	0	790	0.312	0.255	97.34
	1	1566	0.266	0.248	98.66
	2	1561	0.310	0.263	98.65
4.5μm	0	796	0.301	0.260	97.11
	1	1546	0.263	0.244	98.51
	2	1550	0.309	0.266	98.52
5.8μm	0	191	0.327	0.359	93.72
	1	294	0.317	0.378	95.92
	2	289	0.350	0.359	95.85
8.0μm	0	115	0.329	0.382	92.17
	1	93	0.356	0.399	90.32
	2	75	0.447	0.407	88.00

[a] Δ is the separation, in arcsecond, between the matched SAGE-SMC archival sources and the OGLE-III SMC Cepheids.
[b] The standard deviation of the mean.
[c] Fraction of matched SAGE-SMC archival sources within $1''$ radius from the OGLE-III SMC Cepheids.

2 DATA AND EXTINCTION CORRECTION

The photometric mean magnitudes for Cepheids in the SMC at V- and I-bands are taken from OGLE-III (Soszyñski et al. 2010). There are 2626 fundamental (FU) mode and 1644 first-overtone (FO) mode Cepheids in SMC as classified by the OGLE-III survey. We also derive the optical Wesenheit $W_{V,I} = I - 1.55(V - I)$ magnitudes, where the color coefficient is obtained using the extinction law given by Cardelli, Clayton & Mathis (1989). We cross-matched the OGLE-III SMC FO mode Cepheids with the 2MASS point source catalog (Cutri et al. 2003) using a search radius of $2''$ and obtain the corresponding random-phase JHK_S magnitudes. We also cross-matched OGLE-III Cepheids with publicly released SAGE-SMC data and obtain IRAC band photometry upto three epochs. The number of matched sources and the corresponding mean separations and standard deviations are summarized in Table 1 for the SAGE-SMC data. We estimated the error weighted mean if the magnitudes are available for more than one epoch of observation. We find from Table 1 that the majority ($> 95\%$) of matched sources are within $1''$ radius in OGLE-III and SAGE-SMC catalogs. Therefore, the results of our analysis are not affected by the choice of a greater search radius.

We note that near-infrared templates for FO mode Cepheids are not available in literature. Recently, Inno et al. (2015) provided templates for J-band FO mode Cepheids but the calibrator sample was limited to 10 Cepheids in the SMC. Macri et al. (2015) derived new near-infrared PL relations for FO mode Cepheids in the LMC based on the fairly well sampled light curve data for $\sim$ 500 Cepheids. Therefore, we use time series data from Macri et al. (2015) together with the methodology presented in Soszyński, Gieren & Pietrzyński (2005) to correct 2MASS random phase observations to mean magnitudes. We assume negligible effects of metallicity difference on the light curve shape for FO mode Cepheids in the Magellanic Clouds. It is a reasonable assumption considering the fact that FO mode Cepheids have smaller amplitudes and

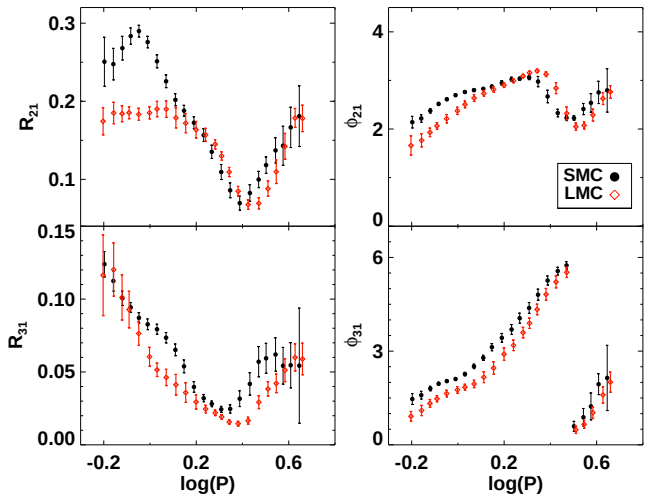

Figure 1. A comparison of mean I-band Fourier parameters for FO mode Cepheids in the Magellanic Clouds. The error bars represent 3σ uncertainties on the mean.

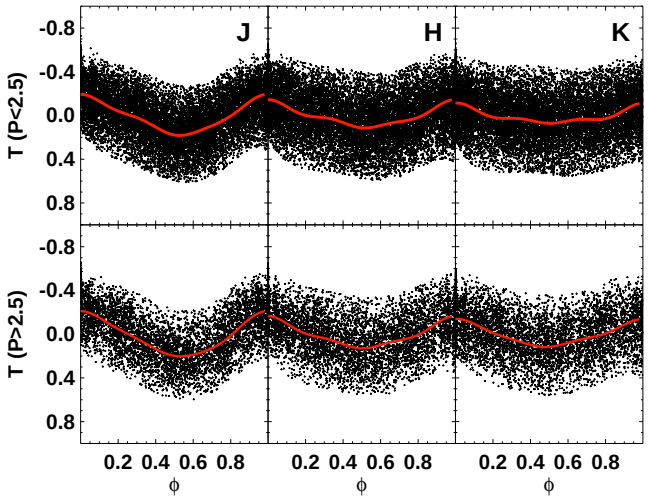

Figure 2. Normalised and merged light curves for LMC FO mode Cepheids in period bins P < 2.5 and P > 2.5 days.

exhibit near sinusoidal light curve structure. A comparison of I-band Fourier parameters for FO mode Cepheids in the Magellanic Clouds is shown in Fig. 1. We use sliding mean calculations with a step size of $\log P = 0.1$ to estimate mean parameters in each period bin (Bhardwaj et al. 2015b). For $\log P > 0.2$, the mean amplitude and phase parameters are consistent between the two clouds. There is a greater difference in Fourier parameters for $\log P < 0.2$ in some period bins but we note that the LMC FO mode Cepheid sample is significantly smaller as compared to SMC in this period range. We also emphasize that for near-infrared light curves, these differences in amplitude and phase parameters will be even smaller.

We normalize each LMC FO mode Cepheid light curve in such a way that the mean magnitude is zero and the amplitude is equal to unity. The Fourier amplitude parameters for FO mode Cepheids show a sharp progression around 2.5 days at optical wavelengths. Therefore, we divided our LMC sample in two period bins and co-added the normalized light curves of each Cepheid in JHK_s bands separately. The plot of merged light curves is shown in Fig. 2. Finally, we fit a third-order Fourier sine series, $T(\phi) = \sum_{i=1}^{3} A_i \sin(2\pi\phi + \Phi_i)$, to the template light curves and obtain amplitude and phase coefficients (Bhardwaj et al. 2015b), listed in Table 2. The amplitude ratios of near-infrared to optical light curves and the phase lag of maximum light between I and JHK_s bands for FO mode Cepheids in the LMC are shown in Fig. 3. We do not find any significant variation of amplitude ratios as a function of period and adopted median values are listed in Table 3. The phase lag for maximum light in JHK_s vs. I for the FO mode Cepheids show a trend as a function of period for P>2.5 days. We note that the J to V-band amplitude ratio (A_J/A_V) for LMC FO mode Cepheids (0.39 for P<2.5 and 0.34 for P>2.5 days) is similar to the SMC FO mode Cepheids from Inno et al. (2015). This is in contrast to fundamental mode Cepheids where the amplitude ratio for SMC Cepheids are significantly smaller than LMC Cepheids, and further suggests that the assumption of similar light curve structure for FO Cepheids in the Magellanic Clouds is a good approximation.

We derive the I-band amplitudes for SMC FO mode Cepheids using full phased light curves from OGLE-III. We use the amplitude ratios for LMC Cepheids together with I-band amplitudes for SMC Cepheids and estimate the amplitude in near-infrared bands for Cepheids in the SMC. Similarly, we calculate the phase of the 2MASS measurement points using the epoch of maximum brightness in I-band from OGLE-III, i.e. $\phi = \mathrm{frac}\left(\frac{JD^{\lambda} - JD^{I}}{P}\right)$. Finally, we calculate the $T(\phi)$ value for this phase and use Fourier coefficients (A_i & Φ_i) together with near-infrared amplitudes to

Table 2. Fourier coefficients for the near-infrared light curves of FO mode Cepheids.

	J-band		H-band		K_s-band	
i	A_i	Φ_i	A_i	Φ_i	A_i	Φ_i
P < 2.5 days						
1	0.171	4.538	0.108	4.586	0.071	4.625
2	0.020	5.410	0.023	5.021	0.027	4.643
3	0.019	4.852	0.023	4.781	0.022	4.699
P > 2.5 days						
1	0.197	4.530	0.128	4.661	0.115	4.728
2	0.025	5.171	0.023	4.831	0.017	4.307
3	0.012	5.174	0.021	4.837	0.013	4.850

Table 3. Near-infrared to optical amplitude ratios for LMC FO mode Cepheids.

P (days)	A_J/A_I	A_H/A_I	A_{K_s}/A_I
all	0.628±0.007	0.417±0.009	0.398±0.008
< 2.5	0.647±0.010	0.413±0.011	0.410±0.011
> 2.5	0.594±0.011	0.413±0.013	0.366±0.011

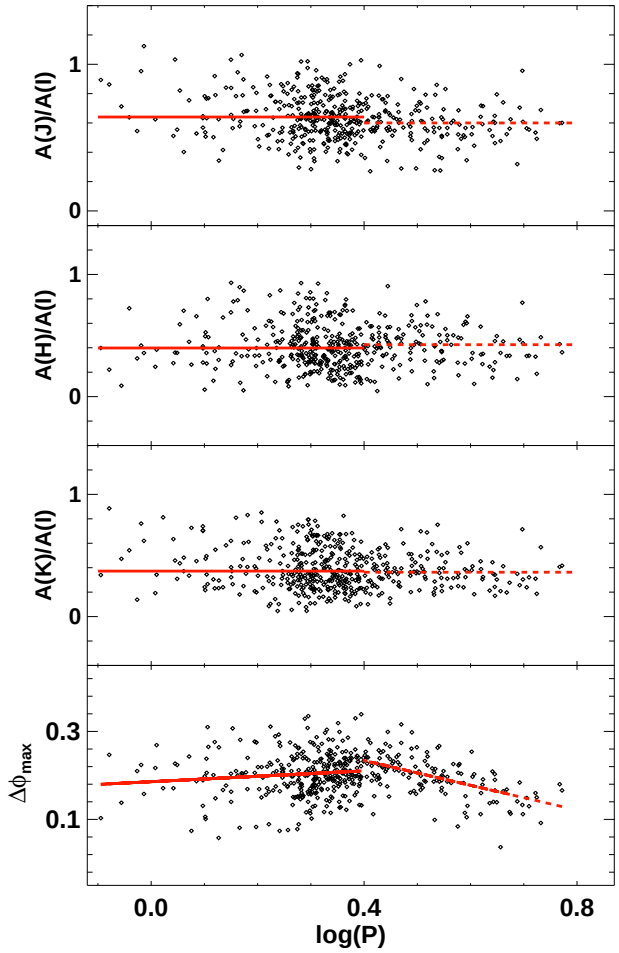

Figure 3. Top three panels represent the optical to near-infrared amplitude ratios for LMC FO mode Cepheids and the bottom panel shows the phase lag between I and JHK_s light curves for LMC Cepheids.

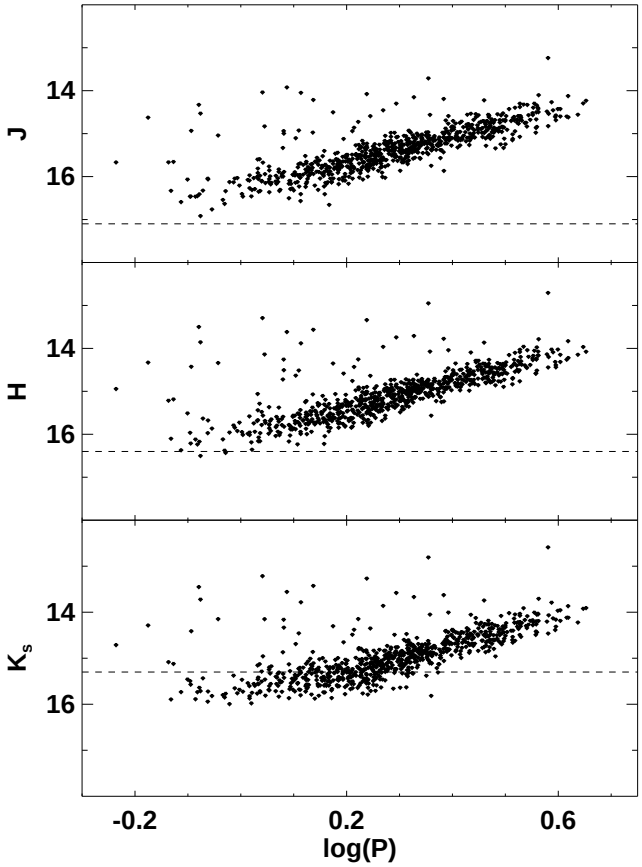

Figure 4. Near-infrared band PL relations for SMC FO mode Cepheids. The dashed lines represent the 2MASS 3σ sensitivity adopted from Cutri et al. (2003).

estimate the mean magnitudes for FO mode Cepheids using $\overline{m(\lambda)} = m(\lambda)_{2MASS} - A(\lambda) \times T(\phi)$. We note that the near-infrared magnitudes from 2MASS have large photometric uncertainties which contribute to the greater dispersion in PL relations. The median uncertainties in the average magnitudes for FO Cepheids in [V, I, J, H, K_s, 3.6μm, 4.5μm] bands range from [0.02, 0.03, 0.06, 0.09, 0.14, 0.06, 0.09] for P<2.5 days to [0.02, 0.03, 0.04, 0.08, 0.08, 0.05, 0.05] for P>2.5 days.

The mean magnitudes for Cepheids in multiple bands are corrected for reddening using Haschke maps (Haschke, Grebel & Duffau 2011). We provide the input locations for OGLE-III Cepheids in terms of RA/DEC and obtain the corresponding E(V-I) color excess. We correct the magnitudes using the extinction law $A_\lambda = R_\lambda E(B-V)$, where E(V-I) is related to E(B-V) by the relation E(V-I) = 1.38 E(B-V) (Tammann, Sandage & Reindl 2003). For the SMC, the values for total-to-selective absorption (R_λ) are $R_{V,\ I,\ J,\ H,\ K,\ 3.6\mu m,\ 4.5\mu m,\ 5.8\mu m,\ 8.0\mu m}$ = {2.40, 1.41, 0.69, 0.43, 0.28, 0.12, 0.09, 0.06, 0.04}, corresponding to E(V-I) color excess (Ngeow et al. 2015).

3 THE PERIOD-LUMINOSITY RELATIONS

Soszyñski et al. (2010) derived the PL and PW relations for FU and FO mode Cepheids in the SMC at optical wavelengths in their data release paper. However, these relations were not corrected for extinction. There are many studies in the past decade on FU mode Cepheid PL relations (for references, see §1) but not for FO mode Cepheids in the Magellanic Clouds. Groenewegen (2000) derived PL relations for FO mode Cepheids by combining OGLE-II data with DENIS and 2MASS infrared data. Bono et al. (2002) carried out a study on theoretical and observed PL relations for FO mode Cepheids in IK_s-bands. A detailed study based on PL and PC relations for SMC Cepheids using OGLE catalogs was carried out by Sandage, Tammann & Reindl (2009) and Tammann, Reindl & Sandage (2011). Recently, Subramanian & Subramaniam (2015) provided new PL relations for FO Cepheids using OGLE-III data and found evidence of several breaks in optical PL and PC relations but no statistical tests were done in their analysis. We extend these studies to derive multi-band PL relations and use our test statistics (Bhardwaj et al. 2016) to rigorously determine any possible non-linearities in these relations for FO mode Cepheids.

Fig. 4 displays near-infrared PL relations using ran-

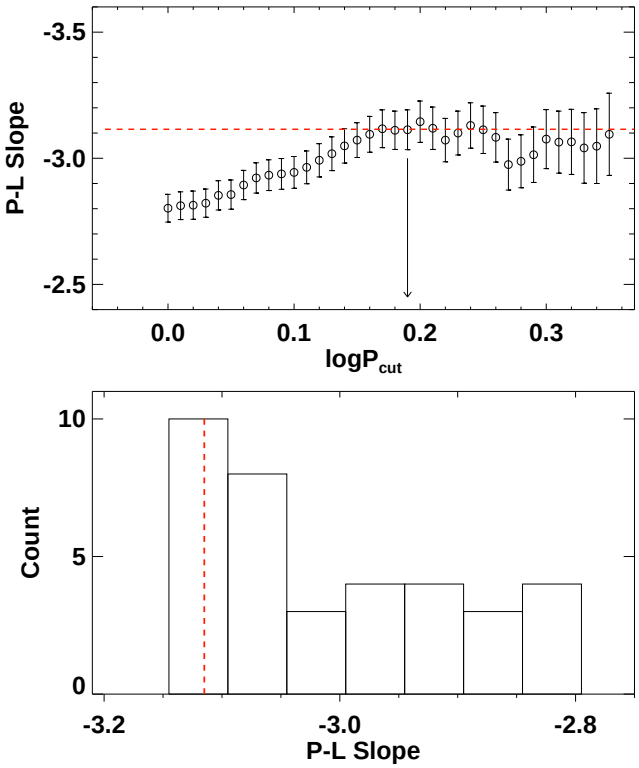

Figure 5. The top panel displays slopes of the fitted PL relations for Cepheids having $\log P > \log P_{cut}$, as a function of the adopted $\log P_{cut}$. The vertical arrow represents the adopted $\log P_{cut}$ in K_s-band. The bottom panel shows the histogram of the distribution of fitted PL slopes. The (red) dashed-lines indicate the mode of the fitted PL slopes based on the histogram.

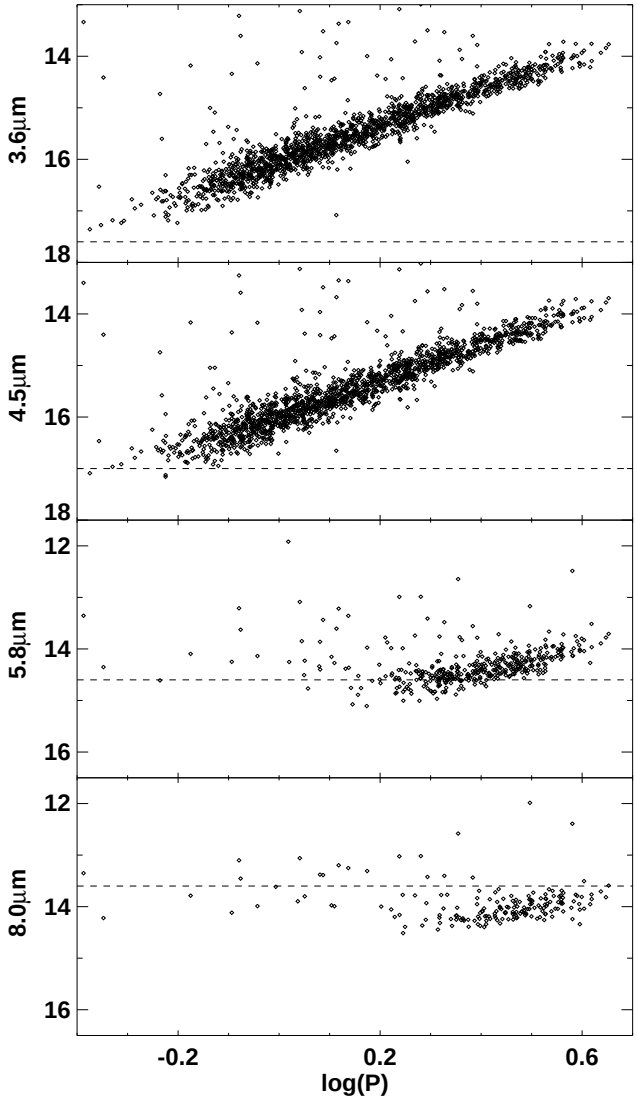

Figure 6. Mid-infrared PL relations for SMC FO mode Cepheids. The dashed lines represent the detection limits in each band for SAGE-SMC catalog.

dom phase corrected mean magnitudes. We find that all J and H-band magnitudes are above the detection limit while the K_s-band magnitudes are influenced due to the incompleteness bias at the short-period end. This incompleteness bias is related to well-known Malmquist bias (see, Sandage 1988, for more details). Therefore, an appropriate period cut is required in K_s-band. We use the method discussed in Ngeow et al. (2015) to adopt period cuts. In brief, we start with an initial $\log P_{cut} = 0$ and fit a PL relation to the remaining sample with iterative 2.5σ clipping and obtain the slope. We repeat this process with a bin size of $\Delta \log P_{cut} = 0.01$ upto a maximum value of $\log P_{cut} = 0.35$. We plot the slopes of the PL relations as a function of $\log P_{cut}$ in the upper panel of Fig. 5 and present these distributions as histograms in the lower panel. We determine the mode of the histogram and the absolute difference between the mode value and the slopes of the PL relations. The $\log P_{cut}$ value corresponding to the smallest absolute difference is adopted as the final period cut for the K_s-band PL relation. Therefore, we adopt the final period cut at $\log P_{cut} = 0.19$ for the K_s-band PL relation. Similarly, Fig. 6 displays the mid-infrared PL relations for FO mode Cepheids. Again, the 3.6μm and 4.5μm band PL relations are not influenced by the incompleteness bias near their detection limit. The magnitudes in 5.8μm and 8.0μm are mostly below the detection limit and therefore, we will not consider these bands further in our analysis.

We make use of extinction corrected mean magnitudes in $VIJHK_s$ & 3.6/4.5μm wavelengths to derive PL relations in each band, separately. At optical and mid-infrared wavelengths, we restrict our sample to $P > 0.6$ days because there are very few stars below this period. Similarly, we only consider stars with $P > 1$ day at near-infrared wavelengths. We apply recursive 2.5σ clipping to fit a PL relation in each band, where σ is the dispersion in the PL relation after each iteration. Stars that are removed because of this procedure may appear as outliers due to several reasons including misidentification in the OGLE-III catalog and blending with nearby sources. Further investigation implies that the majority of these outliers are present in more than one band and therefore should be removed before fitting a

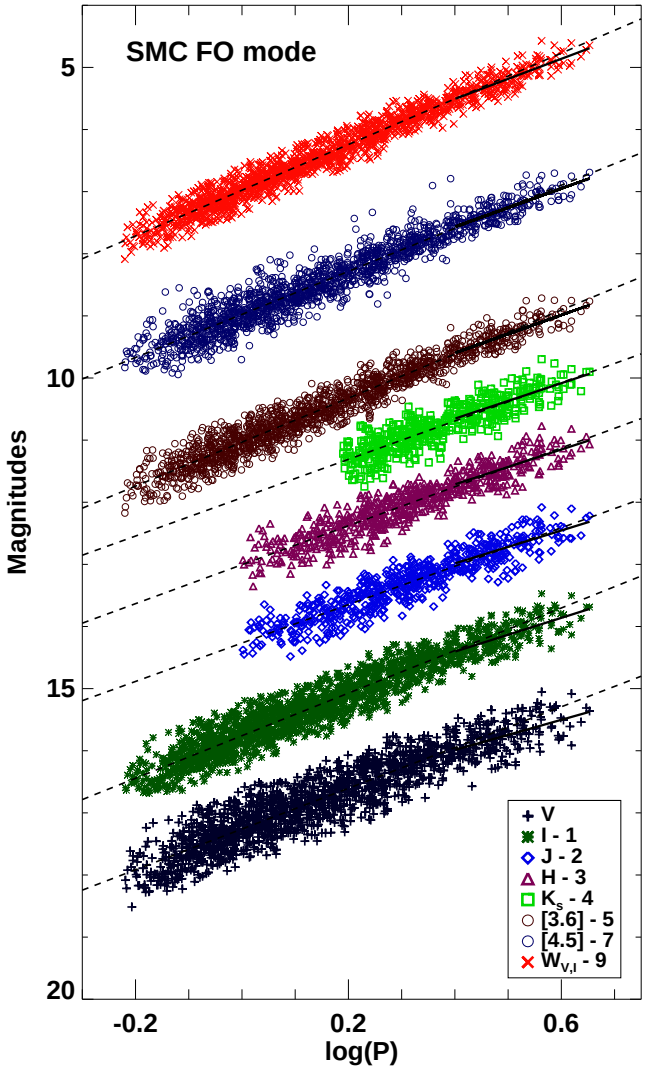

Figure 7. Multi-band PL relations and optical Wesenheit relation for SMC FO mode Cepheids. The solid/dashed lines represent the best fit regression for Cepheids with periods below and above 2.5 days.

PL relation. However, we will not investigate the nature of these outliers in this study. Our final PL relations at multiple bands for the SMC FO mode Cepheids are presented in Fig. 7 and the results are given in Table 4.

We note that the dispersion in the FO mode Cepheid PL relations are very similar to FU mode Cepheid PL relations (Ngeow et al. 2015), except at mid-infrared wavelengths. We do not observe any significant reduction in dispersion of the near-infrared PL relations with or without random phase corrections. For the J-band, the dispersion reduces by ~ 0.01 mag, while it is negligible in the case of H and K_s-band PL relations. We suspect that the dispersion in the 2MASS PL relations is dominated by photometric errors, most likely crowding, and the high intrinsic line-of-sight depth of the SMC (Subramanian & Subramaniam 2015). Hence, phase corrections do not contribute significantly, especially when the pulsation amplitudes are very small. However, the dispersion in the near-infrared PL relation for LMC FO mode Cepheids ranges from 0.09-0.14 mag (Macri et al. 2015) as opposed to 0.18-0.20 mag for SMC FO mode Cepheids. Therefore, we test the contribution of random phase corrections to LMC FO mode Cepheid PL relations. We randomly sample the LMC FO light curves and estimate the dispersion in each band. We find that the random phase PL relations in JHK_s bands do not give significantly different dispersion than the mean light PL relations, specially in H and K_s-bands. The greatest difference of ~ 0.014 mag occurs for J-band in 50 different samples of random PL relations.

Table 4. Multi-band PL relations for SMC FO mode Cepheids.

Band	PL Slope	PL ZP	σ	N
V	-3.147 ± 0.035	17.254 ± 0.008	0.268	1531
I	-3.332 ± 0.028	16.754 ± 0.007	0.218	1531
J	-3.095 ± 0.055	16.267 ± 0.019	0.198	595
H	-3.151 ± 0.053	16.012 ± 0.018	0.191	598
K_s	-3.132 ± 0.083	15.941 ± 0.032	0.197	457
3.6μm	-3.510 ± 0.024	16.030 ± 0.006	0.180	1499
4.5μm	-3.451 ± 0.028	15.975 ± 0.007	0.200	1529
$W_{V,I}$	-3.626 ± 0.020	15.974 ± 0.005	0.153	1526

3.1 Comparison with Published PL Relations

We compare our multi-band PL relations for FO mode Cepheids in the SMC with published results (Bauer et al. 1999; Groenewegen 2000; Soszyñski et al. 2010; Tammann, Reindl & Sandage 2011; Inno et al. 2013; Subramanian & Subramaniam 2015). The optical band PL relations in our study are essentially an updated version of PL relations derived by Soszyñski et al. (2010) as we account for the interstellar extinction. We note that the Wesenheit function, that is independent of the extinction, provides precisely the same slope, as expected, in the two set of PL relations. We use a standard t-test to check the significance of the difference in the slopes of our PL relations with published work. The details of t-test can be found in Ngeow et al. (2015) and Bhardwaj et al. (2015a). In brief, we calculate T-values using the errors on the slopes and the standard deviation of PL relations. The theoretical T-values are obtained from the t-distribution for an adopted significance level ($\alpha = 0.05$), under the null hypothesis of the two slopes being equal. The probability of acceptance of the null hypothesis ($p(t)$) of the observed t-statistic ($|T|$) is listed in Table 5. The null hypothesis that the two slopes under consideration are consistent with each other is rejected if $p(t) < \alpha$.

We find that all PL relations derived in this paper for SMC FO mode Cepheids are consistent with previous studies. At optical wavelengths, the V-band PL relation from Bauer et al. (1999) is derived in the V_{EROS} filter. The PL relations taken from Tammann, Reindl & Sandage (2011) are restricted to the short period range ($\log P < 0.4$), whilst those taken from Subramanian & Subramaniam (2015) are limited to long period ($\log P > 0.029$) FO mode Cepheids in OGLE-III catalog. Similarly, the PL relations adopted

Table 5. Comparison of SMC FO mode PL relations.

PL Slope	σ	N	Src	$\|T\|$	$p(t)$
		V-band			
-3.147±0.035	0.268	1531	TW	—	—
-3.060±0.080	0.250	239	E99	0.948	0.343
-3.171±0.034	0.280	1644	S10	0.491	0.624
-3.203±0.060	0.250	597	T11	0.779	0.436
-3.030±0.056	0.270	1041	S15	1.776	0.076
		I-band			
-3.332±0.028	0.218	1531	TW	—	—
-3.349±0.027	0.230	1644	S10	0.436	0.663
-3.374±0.046	0.190	595	T11	0.728	0.467
-3.230±0.045	0.220	1041	S15	1.930	0.054
		J-band			
-3.095±0.055	0.198	595	TW	—	—
-3.104±0.159	0.183	158	G00	0.094	0.926
		H-band			
-3.151±0.053	0.191	598	TW	—	—
-3.199±0.142	0.162	162	G00	0.316	0.754
		K_s-band			
-3.132±0.083	0.197	457	TW	—	—
-3.102±0.155	0.178	156	G00	0.136	0.887
		$W_{V,I}$			
-3.626±0.020	0.153	1526	TW	—	—
-3.558±0.025	0.126	688	G00	1.972	0.049
-3.623±0.020	0.160	1644	S10	0.106	0.915
-3.599±0.027	0.140	1465	I13	0.790	0.430

Notes: Source : TW - this work; E99 - Bauer et al. (EROS collaboration, 1999); G00 - Groenewegen (2000); S10 - Soszyński et al. (2010); T11 - Tammann, Reindl & Sandage (2011); I13 - Inno et al. (2013); S15 - Subramanian & Subramaniam (2015).

from Groenewegen (2000), derived using 2MASS and DENIS data, are limited to long period ($\log P > 0.3$) Cepheids only. For each set of slopes under consideration, the t-test suggests that the data are consistent with the null hypothesis at the 95% significance level. Therefore, the corresponding set of slopes are equal within their quoted uncertainties. The slope of the Wesenheit function derived by Groenewegen (2000) is marginally inconsistent according to the t-test, presumably due to a significantly smaller sample size of OGLE-II Cepheids as compared to OGLE-III.

3.2 A Test for Non-Linearity in PL Relations

Non-linearity in the PL relations for Cepheids in the LMC is discussed in detail in Bhardwaj et al. (2016). The LMC FU mode Cepheid PL relations exhibit a break at 10 days at optical and near-infrared wavelengths and the FO mode Cepheids provide evidence of a break in the PL relation at 2.5 days only at optical wavelengths. However, Ngeow et al. (2015) suggest there is no break in the SMC FU mode Cepheid PL relations at 10 days, if we do not consider stars with periods below 2.5 days. Further, Subramanian & Subramaniam (2015) found a break in the PL relations of both the FU and FO mode Cepheids at $P \sim 2.95$ days and $P \sim 1$ day, respectively. Subramanian & Subramaniam (2015) did not use any statistical tests to determine the significance of these observed breaks. We will test for any possible statistically significant non-linearity in SMC FO mode Cepheid PL relations using robust statistical tests such as the F-test, random walk method and the testimator. These test statistics are discussed in detail in Bhardwaj et al. (2016) and will not be repeated here. In brief, the F-test compares a single regression line model over the entire period range with a two line regression, under the null hypothesis that the data follows a linear model. The random walk is a non-parametric test and uses the partial sum of random permutation of residuals to test any departure from linearity. The testimator compares the slopes of a number of subsets of the data to find evidence of change in the slope of the PL relation.

The results of the F-test, random walk and the testimator analysis are provided in Table 6 and 7. We test for non-linearity in the PL relations at 2.5 days and 1 day following the observed breaks in the PC (Bhardwaj et al. 2014) and PL relations (Subramanian & Subramaniam 2015), respectively. At optical wavelengths, PL and PW relations provide evidence for a significant break at both 2.5 days and 1 day, according to all test statistics. The results of all the test statistics imply that we can reject the null hypothesis that a single regression line is a better model at a very high significance level. However, we do not find any significant change in the slope of PL relations at these periods in infrared bands. We use our tests to determine the significance of the break at 1.6 days, which is related to a feature in Fourier parameters for SMC FO mode Cepheids. The F-test and random walk find evidence of a significant break at 1.6 days in PL and PW relations. Independently, the testimator suggests a break in the PL and PW relations in a bin including 2.5 days period.

We note that Subramanian & Subramaniam (2015) found evidence of a break at 1 day. The assumed break point at 2.5 days and 1.6 days are related to non-linearities in PC relations at various phases of pulsation and also with sharp changes in light curve parameters for FO mode Cepheids (Bhardwaj et al. 2014). In order to find the most dominant break point in optical band PL and PW relations, we apply period-cuts before using test statistics. If we consider stars with $P > 1$ day in our analysis, we still find significant change in the slope of the optical band relations at 2.5 days. However, if we only consider stars with $P < 2.5$ days, we do not find evidence of a non-linearity at 1 day in I-band PL and the Wesenheit relation. While the F-test suggests a break in the V-band PL relation, the random walk test does not support this non-linearity. Therefore, we emphasize that the non-linearity observed at 1 day in Subramanian & Subramaniam (2015) is influenced by the change in slope of PL relations for P> 2.5 days. Thus, the most dominant break in FO mode Cepheid PL relations at optical bands occurs at 2.5 days, similar to FU mode Cepheids.

Fig. 8 presents the light curve parameters for FU and FO mode Cepheids in the SMC. The top panel displays the I-band Fourier amplitude parameter (Bhardwaj et al. 2015b) for FU mode Cepheids. We observe a maxima around

Table 6. Results of F and random walk tests for PL, PW and PC relations for FO mode Cepheids in the SMC to test for non-linearity at various periods.

Y	PL Slope$_S$	PL ZP$_S$	σ_S	N_S	PL Slope$_L$	PL ZP$_L$	σ_S	N_S	F	$p(F)$	$p(R)$
For all P with a break at 2.5 days (Bhardwaj et al. 2014)											
V	-3.279±0.046	17.260±0.008	0.268	1349	-2.426±0.303	16.957±0.149	0.244	182	11.104	0.000	0.002
I	-3.427±0.038	16.758±0.007	0.219	1348	-2.718±0.243	16.492±0.119	0.197	183	9.075	0.000	0.010
J	-3.092±0.094	16.266±0.024	0.197	423	-2.649±0.254	16.043±0.125	0.198	172	1.599	0.203	0.278
H	-3.136±0.093	16.005±0.024	0.195	426	-2.803±0.231	15.833±0.114	0.181	172	1.064	0.346	0.430
K_s	-3.086±0.212	15.927±0.064	0.204	285	-2.854±0.236	15.796±0.116	0.184	172	0.725	0.485	0.391
3.6μm	-3.544±0.033	16.032±0.006	0.185	1309	-3.052±0.181	15.817±0.089	0.146	190	3.013	0.049	0.573
4.5μm	-3.466±0.038	15.976±0.007	0.208	1339	-3.085±0.178	15.800±0.087	0.145	190	1.091	0.336	0.224
$W_{V,I}$	-3.676±0.027	15.977±0.005	0.154	1335	-3.229±0.175	15.799±0.086	0.143	191	5.642	0.004	0.016
$V-I$	0.157±0.011	0.503±0.002	0.064	1339	0.377±0.073	0.426±0.036	0.058	181	13.915	0.000	0.000
For all P with a break at 1 day (Subramanian & Subramaniam 2015)											
V	-3.868±0.246	17.218±0.023	0.277	419	-3.015±0.049	17.216±0.014	0.262	1112	9.956	0.000	0.001
I	-3.677±0.205	16.743±0.019	0.229	419	-3.241±0.040	16.727±0.011	0.212	1112	5.666	0.004	0.011
3.6μm	-3.510±0.191	16.035±0.018	0.210	404	-3.487±0.032	16.023±0.009	0.169	1095	0.451	0.637	0.576
4.5μm	-3.129±0.220	15.998±0.021	0.237	413	-3.473±0.038	15.981±0.010	0.186	1116	1.573	0.208	0.221
$W_{V,I}$	-3.607±0.150	15.988±0.014	0.170	415	-3.567±0.028	15.956±0.008	0.147	1111	3.969	0.019	0.014
$V-I$	-0.048±0.061	0.485±0.006	0.069	418	0.219±0.012	0.494±0.003	0.060	1102	12.427	0.000	0.000
For all P with a break at 1.6 days, related to a feature in Fourier parameters (see, Fig. 8 in Bhardwaj et al. 2014)											
V	-3.342±0.084	17.259±0.009	0.273	956	-2.805±0.098	17.132±0.036	0.253	575	8.472	0.000	0.001
I	-3.443±0.069	16.758±0.007	0.224	958	-3.058±0.078	16.653±0.029	0.204	573	6.902	0.001	0.011
J	-2.497±0.314	16.202±0.042	0.207	146	-3.053±0.084	16.247±0.032	0.194	449	2.335	0.098	0.269
H	-2.668±0.319	15.951±0.043	0.211	147	-3.155±0.079	16.008±0.031	0.184	451	1.386	0.251	0.421
K_s	-11.005±12.711	17.365±2.482	0.138	10	-3.163±0.085	15.951±0.033	0.197	447	1.790	0.168	0.397
3.6μm	-3.498±0.061	16.033±0.006	0.194	928	-3.389±0.061	15.982±0.023	0.157	571	1.842	0.159	0.573
4.5μm	-3.316±0.071	15.978±0.007	0.220	947	-3.368±0.071	15.936±0.026	0.165	582	3.581	0.028	0.237
$W_{V,I}$	-3.678±0.049	15.977±0.005	0.160	948	-3.452±0.055	15.909±0.020	0.141	578	5.184	0.006	0.015
$V-I$	0.139±0.020	0.502±0.002	0.066	952	0.279±0.023	0.470±0.008	0.058	568	10.083	0.000	0.000
For $P>1$ day with a break at 2.5 days											
V	-3.178±0.075	17.240±0.016	0.263	930	-2.426±0.303	16.957±0.149	0.244	182	5.415	0.005	0.054
I	-3.364±0.061	16.745±0.013	0.214	929	-2.718±0.243	16.492±0.119	0.197	183	5.082	0.006	0.056
J	-3.092±0.094	16.266±0.024	0.197	423	-2.649±0.254	16.043±0.125	0.198	172	1.599	0.203	0.271
H	-3.136±0.093	16.005±0.024	0.195	426	-2.803±0.231	15.833±0.114	0.181	172	1.064	0.346	0.432
K_s	-3.086±0.212	15.927±0.064	0.204	285	-2.854±0.236	15.796±0.116	0.184	172	0.725	0.485	0.387
3.6μm	-3.542±0.051	16.032±0.011	0.174	904	-3.052±0.181	15.817±0.089	0.146	190	2.926	0.054	0.166
4.5μm	-3.538±0.060	15.991±0.013	0.194	925	-3.085±0.178	15.800±0.087	0.145	190	2.092	0.124	0.151
$W_{V,I}$	-3.628±0.043	15.965±0.009	0.147	920	-3.229±0.175	15.799±0.086	0.143	191	3.119	0.045	0.062
$V-I$	0.168±0.017	0.501±0.004	0.060	921	0.377±0.073	0.426±0.036	0.058	181	9.050	0.000	0.001
For $P<2.5$ days with a break at 1 day											
V	-3.868±0.246	17.218±0.023	0.277	419	-3.178±0.075	17.240±0.016	0.263	930	4.023	0.018	0.127
I	-3.677±0.205	16.743±0.019	0.229	419	-3.364±0.061	16.745±0.013	0.214	929	1.434	0.239	0.568
3.6μm	-3.512±0.190	16.035±0.018	0.210	405	-3.542±0.051	16.032±0.011	0.174	904	0.020	0.980	0.701
4.5μm	-3.135±0.220	15.998±0.021	0.237	414	-3.538±0.060	15.991±0.013	0.194	925	2.146	0.117	0.128
$W_{V,I}$	-3.607±0.150	15.988±0.014	0.170	415	-3.628±0.043	15.965±0.009	0.147	920	1.192	0.304	0.609
$V-I$	-0.048±0.061	0.485±0.006	0.069	418	0.168±0.017	0.501±0.004	0.060	921	6.797	0.001	0.011

Notes: The subscripts S and L stand for short and long period range, respectively, for a given break period. ZP and σ represents the zero point and dispersion of the PL relation, respectively. N is the number of Cepheids used in deriving the PL relations. $p(F)$ and $p(R)$ represent the probability of acceptance of the null hypothesis i.e. linear relation.

2.5 days in R_{21} parameter as a function of period. The shorter period Cepheids ($P<2.5$ days) in the SMC occupy a different location such that stars with lower periods have smaller amplitude ratio. The middle panel displays the Fourier amplitude parameter for FO mode Cepheids. This parameter clearly exhibits a sharp change in the progression with period around $\log P = 0.4$. There is also a break around $P = 1.6$ days. All these changes in the progressions are also visible in other amplitude and phase parameters. The bottom panel presents the variation of the third principal com-

Table 7. Results of the testimator on PL, PW and PC relations for FO mode Cepheids in the SMC.

Band	n	$\log(P)$	N	$\hat{\beta}$	β_0	$\lvert t_{obs}\rvert$	t_c	k	Decision	β_w
V	1	-0.21900−-0.07000	208	-4.179 ± 0.491	—	—	—	—	—	—
	2	-0.07000−0.00100	211	-3.069 ± 0.917	-4.179	1.210	2.717	0.446	Accept H_0	-3.685
	3	0.00100−0.07100	210	-2.834 ± 0.964	-3.685	0.883	2.717	0.325	Accept H_0	-3.408
	4	0.07100−0.15000	209	-3.144 ± 0.739	-3.408	0.358	2.717	0.132	Accept H_0	-3.373
	5	0.15000−0.24600	211	-3.637 ± 0.656	-3.373	0.403	2.717	0.148	Accept H_0	-3.412
	6	0.24600−0.34200	211	-3.710 ± 0.615	-3.412	0.484	2.717	0.178	Accept H_0	-3.465
	7	0.34200−0.65300	270	-2.428 ± 0.191	-3.465	5.421	2.711	2.000	Reject H_0	-1.390
I	1	-0.21900−-0.07000	207	-3.891 ± 0.407	—	—	—	—	—	—
	2	-0.07000−0.00100	212	-2.904 ± 0.772	-3.891	1.278	2.716	0.471	Accept H_0	-3.427
	3	0.00100−0.07100	210	-3.349 ± 0.791	-3.427	0.099	2.717	0.036	Accept H_0	-3.424
	4	0.07100−0.15000	208	-3.564 ± 0.593	-3.424	0.236	2.717	0.087	Accept H_0	-3.436
	5	0.15000−0.24600	212	-4.021 ± 0.544	-3.436	1.076	2.716	0.396	Accept H_0	-3.668
	6	0.24600−0.34200	211	-3.755 ± 0.490	-3.668	0.178	2.717	0.066	Accept H_0	-3.673
	7	0.34200−0.65300	270	-2.795 ± 0.154	-3.673	5.689	2.711	2.099	Reject H_0	-1.830
J	1	0.00200−0.16800	110	-2.476 ± 0.423	—	—	—	—	—	—
	2	0.16800−0.25600	110	-4.242 ± 0.745	-2.476	2.369	2.621	0.904	Accept H_0	-4.072
	3	0.25600−0.32600	108	-3.960 ± 0.851	-4.072	0.132	2.622	0.050	Accept H_0	-4.066
	4	0.32600−0.41800	112	-3.838 ± 0.588	-4.066	0.389	2.620	0.148	Accept H_0	-4.032
	5	0.41800−0.65300	154	-2.704 ± 0.299	-4.032	4.444	2.608	1.704	Reject H_0	-1.769
H	1	0.00200−0.16700	109	-2.600 ± 0.444	—	—	—	—	—	—
	2	0.16700−0.25500	110	-3.692 ± 0.755	-2.600	1.446	2.621	0.552	Accept H_0	-3.202
	3	0.25500−0.32500	111	-3.785 ± 0.815	-3.202	0.715	2.621	0.273	Accept H_0	-3.361
	4	0.32500−0.41500	110	-2.984 ± 0.555	-3.361	0.679	2.621	0.259	Accept H_0	-3.264
	5	0.41500−0.65300	157	-2.921 ± 0.264	-3.264	1.296	2.608	0.497	Accept H_0	-3.093
K_s	1	0.19000−0.26000	90	-2.727 ± 1.184	—	—	—	—	—	—
	2	0.26000−0.32000	90	-5.291 ± 1.097	-2.727	2.337	2.632	0.888	Accept H_0	-5.004
	3	0.32000−0.38700	89	-0.508 ± 0.958	-5.004	4.691	2.632	1.782	Reject H_0	3.008
3.6μm	1	-0.22000−-0.06500	209	-3.436 ± 0.359	—	—	—	—	—	—
	2	-0.06500−0.00800	211	-2.501 ± 0.677	-3.436	1.381	2.717	0.509	Accept H_0	-2.960
	3	0.00800−0.07700	207	-3.714 ± 0.665	-2.960	1.132	2.717	0.417	Accept H_0	-3.274
	4	0.07700−0.16100	212	-4.383 ± 0.481	-3.274	2.307	2.716	0.849	Accept H_0	-4.216
	5	0.16100−0.25500	209	-4.074 ± 0.443	-4.216	0.320	2.717	0.118	Accept H_0	-4.199
	6	0.25500−0.36300	212	-3.588 ± 0.322	-4.199	1.898	2.716	0.699	Accept H_0	-3.772
	7	0.36300−0.65300	238	-3.204 ± 0.148	-3.772	3.835	2.714	1.413	Reject H_0	-2.970
4.5μm	1	-0.22000−-0.06600	210	-2.695 ± 0.416	—	—	—	—	—	—
	2	-0.06600−0.00300	209	-2.120 ± 0.827	-2.695	0.695	2.717	0.256	Accept H_0	-2.548
	3	0.00300−0.07300	211	-3.710 ± 0.812	-2.548	1.432	2.717	0.527	Accept H_0	-3.160
	4	0.07300−0.15400	210	-4.139 ± 0.575	-3.160	1.701	2.717	0.626	Accept H_0	-3.773
	5	0.15400−0.24800	209	-3.898 ± 0.512	-3.773	0.245	2.717	0.090	Accept H_0	-3.784
	6	0.24800−0.34900	211	-4.420 ± 0.423	-3.784	1.503	2.717	0.553	Accept H_0	-4.136
	7	0.34900−0.65300	268	-3.211 ± 0.140	-4.136	6.593	2.711	2.432	Reject H_0	-1.886
$W_{V,I}$	1	-0.22000−-0.06700	210	-3.955 ± 0.289	—	—	—	—	—	—
	2	-0.06700−0.00200	207	-2.933 ± 0.591	-3.955	1.728	2.717	0.636	Accept H_0	-3.305
	3	0.00200−0.07300	209	-3.514 ± 0.521	-3.305	0.400	2.717	0.147	Accept H_0	-3.336
	4	0.07300−0.15500	214	-4.135 ± 0.399	-3.336	2.003	2.716	0.737	Accept H_0	-3.925
	5	0.15500−0.25000	209	-4.007 ± 0.404	-3.925	0.205	2.717	0.075	Accept H_0	-3.931
	6	0.25000−0.35100	211	-4.005 ± 0.308	-3.931	0.241	2.717	0.089	Accept H_0	-3.938
	7	0.35100−0.65300	265	-3.451 ± 0.120	-3.938	4.049	2.711	1.493	Reject H_0	-3.212
$V-I$	1	-0.21900−-0.06800	210	-0.034 ± 0.130	—	—	—	—	—	—
	2	-0.06800−0.00200	210	-0.046 ± 0.209	-0.034	0.056	2.717	0.021	Accept H_0	-0.034
	3	0.00200−0.07200	207	0.216 ± 0.216	-0.034	1.157	2.717	0.426	Accept H_0	0.072
	4	0.07200−0.15000	210	0.194 ± 0.181	0.072	0.668	2.717	0.246	Accept H_0	0.102
	5	0.15000−0.24700	213	0.151 ± 0.148	0.102	0.333	2.716	0.122	Accept H_0	0.108
	6	0.24700−0.34900	210	0.041 ± 0.139	0.108	0.480	2.717	0.177	Accept H_0	0.096
	7	0.34900−0.65300	259	0.394 ± 0.047	0.096	6.332	2.712	2.335	Reject H_0	0.791

Notes: The meaning of each column header - n represents the number of non-overlapping subsets and $\log(P)$ is the period range in each subset. N and $\hat{\beta}$ represent the number of stars and slope of linear regression in each subset, respectively. β_0 and β_w represent the initial and updated testimator slope after each hypothesis testing. $|t_{obs}|$ is estimated using errors on the slopes and the standard deviation of PL relations and t_c represents the theoretical T-value for confidence level of more than 95%. k is the probability of initial guess of the testimator being true and leads to the decision of acceptance/rejection.

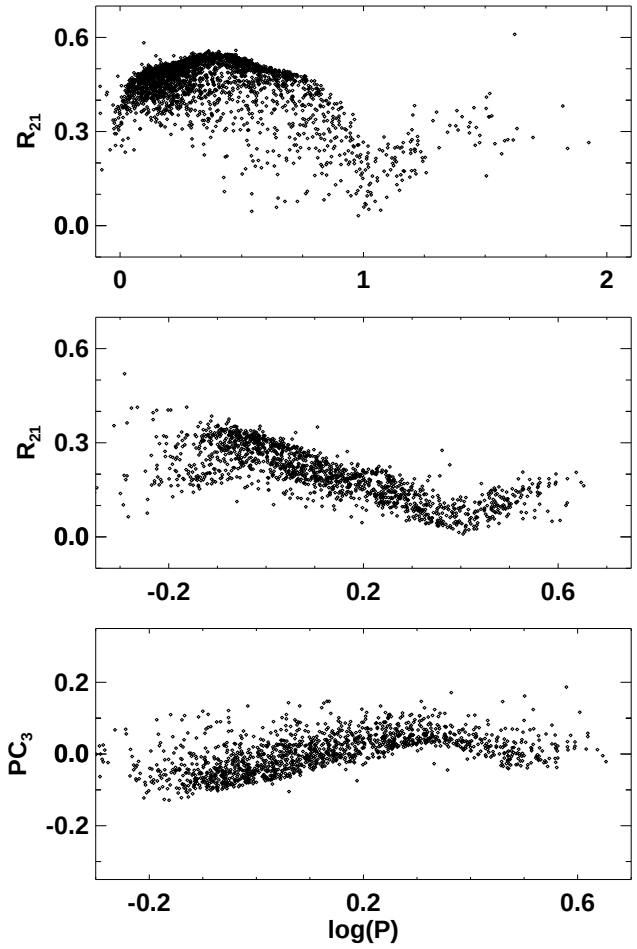

Figure 8. Light curve parameters for FU and FO mode Cepheids in the SMC. The top panel displays the I-band Fourier amplitude parameter (Bhardwaj et al. 2015b) for FU mode Cepheids. The middle panel shows Fourier amplitude parameter for FO mode Cepheids. The bottom panel shows the variation of the third principal component (Deb & Singh 2009) of I-band light curves of SMC FO mode Cepheids.

ponent (Deb & Singh 2009) obtained from the I-band light curves of SMC FO mode Cepheids. Again, a change in the progression around $\log P = 0.4$ is distinctly observed and similar but less pronounced features are seen in first and second principal components. Our test statistics results provide clear evidence that the observed non-linearities are related to changes in light curve structure.

We also test the robustness of our test statistics results under various assumptions such as, homoscedasticity, independent and identically distributed variables and normality of residuals. The observations of Cepheids are independent of each other and the average of PL residuals do not show any significant trend as a function of period. Further, the mean of PL residuals is close to zero and the majority of the residuals follow a normal distribution. We also use quantile-quantile (q-q) plots to find the outliers at the extreme ends and tested whether our results are sensitive to these outliers. The robustness of F-test under these assumptions is discussed in detail in Ngeow et al. (2015) and Bhardwaj et al. (2016). However, our results are robust to these assumptions and are supported by non-parametric random walk test.

Table 8. Multi-band PL relations for SMC FU mode Cepheids.

Band	PL Slope	PL ZP	σ	N
V	-2.919±0.018	17.892±0.008	0.254	2487
I	-3.133±0.014	17.349±0.007	0.204	2477
J	-3.149±0.016	16.861±0.008	0.213	2150
H	-3.082±0.020	16.482±0.010	0.246	2114
3.6μm	-3.381±0.013	16.554±0.006	0.179	2443
4.5μm	-3.343±0.014	16.497±0.006	0.191	2449
$W_{V,I}$	-3.468±0.010	16.501±0.005	0.142	2466

4 A COMPARISON WITH SHORT PERIOD FUNDAMENTAL-MODE CEPHEIDS

Ngeow et al. (2015) derived the multi-band PL relations for SMC FU mode Cepheids with $P > 2.5$ days. Therefore, in our analysis we include the short period Cepheids to compare with FO mode Cepheids and simultaneously test for any evidence of a possible non-linearity in PL, PW and PC relations at short periods. The short period breaks of around 2 days in the PL relation for FU mode SMC Cepheids was first reported by Bauer et al. (1999) and further revisited by Sandage, Tammann & Reindl (2009, at 2.5 days). Bhardwaj et al. (2014) discussed these breaks in PC & A-C relations as a function of pulsation phase at 2.5 days. However, Subramanian & Subramaniam (2015) found a break in PL and PC relations for FU mode Cepheids at 2.95 days. In our analysis, we make use of OGLE-III counterparts for FU mode Cepheids in 2MASS and SAGE-SMC catalogs, taken from Ngeow et al. (2015). We use extinction corrected mean magnitudes and apply 2.5σ clipping to fit PL, PW and PC relations. The results of a single regression line over the entire period range are provided in Table 8. We note that these PL relations are significantly different to Ngeow et al. (2015) results, presumably due to inclusion of short period ($P < 2.5$ days) Cepheids.

The plots of multi-band PL relations and optical Wesenheit for FU mode Cepheids are displayed in Fig. 9. The results of the F-test, Random Walk and the testimator analysis are provided in Table 9 and 10, respectively. Ngeow et al. (2015) found that the K_s, 5.8 & 8.0μm bands PL relations are influenced by the incompleteness at short period ends and, therefore, required a period cut. Hence, we do not use these bands in our study of short period breaks in PL relations. The optical V- and I-band PL relations and the Wesenheit function for SMC FU mode Cepheids provide evidence for a significant variation in slope between Cepheids having periods smaller/greater than 2.5 days. Similarly, the near-infrared (J & H) and mid-infrared (3.6 & 4.5μm) band PL relations also provide evidence for a very large deviation in slope for short and long period range Cepheids. Visual inspection of H-band PL relation from Ngeow et al. (2015) suggests that the magnitudes may be approaching incompleteness limit at the short period end leading to a large deviation in slope. However, the magnitudes in other infrared bands lie well above their detection limit and, there-

Table 9. Results of F and random walk tests for PL and PW and PC relations for FU mode Cepheids in the SMC to test non-linearity at various periods. The meaning of each column header is discussed in Table 6.

Y	PL Slope$_S$	PL ZP$_S$	σ_S	N_S	PL Slope$_L$	PL ZP$_L$	σ_S	N_S	F	$p(F)$	$p(R)$
For all P with a break at 2.5 days (Bhardwaj et al. 2014)											
V	-3.057±0.064	17.935±0.015	0.243	1567	-2.678±0.035	17.704±0.025	0.261	920	34.865	0.000	0.000
I	-3.267±0.052	17.389±0.012	0.195	1557	-2.930±0.028	17.192±0.020	0.208	920	38.858	0.000	0.000
J	-2.732±0.068	16.783±0.016	0.216	1246	-3.059±0.028	16.779±0.020	0.199	904	32.633	0.000	0.000
H	-2.281±0.086	16.307±0.021	0.266	1197	-3.156±0.030	16.523±0.021	0.202	917	54.788	0.000	0.000
3.6μm	-3.519±0.049	16.588±0.011	0.185	1532	-3.242±0.024	16.449±0.017	0.164	911	21.795	0.000	0.000
4.5μm	-3.375±0.052	16.513±0.012	0.199	1531	-3.196±0.025	16.382±0.018	0.172	918	20.144	0.000	0.000
$W_{V,I}$	-3.588±0.037	16.534±0.008	0.136	1542	-3.323±0.020	16.388±0.014	0.144	924	41.961	0.000	0.000
$V-I$	0.206±0.016	0.549±0.004	0.060	1562	0.272±0.009	0.503±0.006	0.066	911	23.729	0.000	0.000
For all P with a break at 2.95 days (Subramanian & Subramaniam 2015)											
V	-3.176±0.052	17.955±0.013	0.245	1731	-2.689±0.040	17.714±0.031	0.262	756	30.706	0.000	0.000
I	-3.352±0.042	17.403±0.011	0.196	1719	-2.932±0.032	17.194±0.024	0.208	758	35.979	0.000	0.000
J	-3.015±0.053	16.836±0.014	0.219	1406	-3.063±0.032	16.784±0.024	0.197	744	9.500	0.000	0.000
H	-2.621±0.067	16.372±0.018	0.266	1360	-3.165±0.033	16.530±0.025	0.197	754	31.238	0.000	0.000
3.6μm	-3.560±0.039	16.595±0.010	0.183	1694	-3.250±0.027	16.457±0.020	0.163	749	21.470	0.000	0.000
4.5μm	-3.455±0.041	16.526±0.011	0.197	1693	-3.195±0.028	16.382±0.021	0.170	756	16.467	0.000	0.000
$W_{V,I}$	-3.641±0.030	16.543±0.008	0.137	1705	-3.324±0.022	16.390±0.017	0.144	761	39.886	0.000	0.000
$V-I$	0.175±0.013	0.554±0.003	0.061	1724	0.269±0.010	0.505±0.008	0.066	749	19.303	0.000	0.000

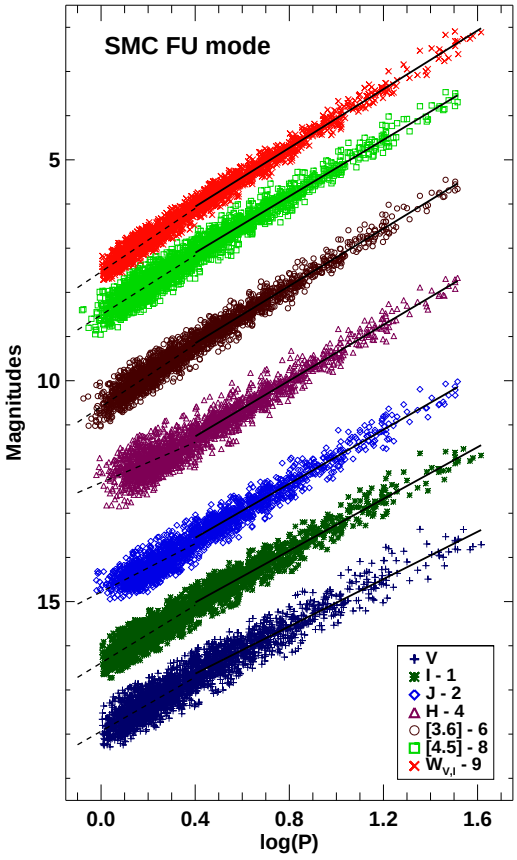

Figure 9. Multi-band PL relations and optical Wesenheit relation for SMC FU mode Cepheids. The solid/dashed lines represent the best fit regression for Cepheids with periods below and above 2.5 days.

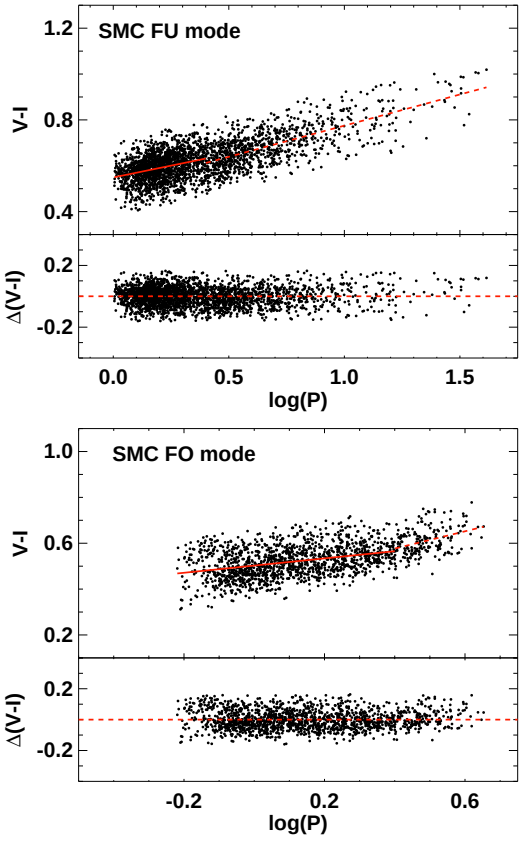

Figure 10. Optical-band PC relation for SMC FU and FO mode Cepheids. The solid/dashed lines represent the best fit regression for Cepheids with periods below and above 2.5 days. The residuals from a single regression line are shown in the bottom panels.

Table 10. Results of the testimator on PL, PW and PC relations for FU mode Cepheids in the SMC. The meaning of each column header is discussed in Table 7.

Band	n	log(P)	N	$\hat{\beta}$	β_0	$\lvert t_{obs}\rvert$	t_c	k	Decision	β_w
V	1	0.00500−0.11100	269	-3.178 ± 0.530	—	—	—	—	—	—
	2	0.11100−0.16200	269	-3.890 ± 1.014	-3.178	0.703	2.795	0.251	Accept H_0	-3.357
	3	0.16200−0.20700	267	-3.910 ± 1.030	-3.357	0.537	2.796	0.192	Accept H_0	-3.463
	4	0.20700−0.25700	274	-2.627 ± 1.001	-3.463	0.835	2.795	0.299	Accept H_0	-3.213
	5	0.25700−0.31800	270	-5.124 ± 0.780	-3.213	2.449	2.795	0.876	Accept H_0	-4.887
	6	0.31800−0.42100	271	-4.628 ± 0.565	-4.887	0.459	2.795	0.164	Accept H_0	-4.845
	7	0.42100−0.53300	270	-2.520 ± 0.491	-4.845	4.732	2.795	1.693	Reject H_0	-0.909
I	1	0.00500−0.11100	268	-3.539 ± 0.449	—	—	—	—	—	—
	2	0.11100−0.16300	270	-4.097 ± 0.813	-3.539	0.686	2.795	0.245	Accept H_0	-3.676
	3	0.16300−0.20800	271	-3.581 ± 0.819	-3.676	0.116	2.795	0.042	Accept H_0	-3.672
	4	0.20800−0.26000	271	-2.089 ± 0.792	-3.672	1.998	2.795	0.715	Accept H_0	-2.540
	5	0.26000−0.32200	270	-4.336 ± 0.614	-2.540	2.923	2.795	1.046	Reject H_0	-4.418
J	1	-0.02000−0.14000	227	-1.474 ± 0.352	—	—	—	—	—	—
	2	0.14000−0.19000	226	-2.402 ± 0.951	-1.474	0.976	2.800	0.349	Accept H_0	-1.797
	3	0.19000−0.23600	235	-2.807 ± 1.024	-1.797	0.986	2.799	0.352	Accept H_0	-2.153
	4	0.23600−0.28700	229	-3.820 ± 0.914	-2.153	1.823	2.799	0.651	Accept H_0	-3.238
	5	0.28700−0.36300	233	-3.118 ± 0.690	-3.238	0.175	2.799	0.062	Accept H_0	-3.231
	6	0.36300−0.46000	228	-4.394 ± 0.480	-3.231	2.423	2.800	0.866	Accept H_0	-4.238
	7	0.46000−0.56100	232	-2.070 ± 0.445	-4.238	4.867	2.799	1.739	Reject H_0	-0.468
H	1	-0.02000−0.14700	230	-1.235 ± 0.528	—	—	—	—	—	—
	2	0.14700−0.19800	229	0.327 ± 1.329	-1.235	1.176	2.799	0.420	Accept H_0	-0.579
	3	0.19800−0.24400	228	-2.564 ± 1.330	-0.579	1.492	2.800	0.533	Accept H_0	-1.637
	4	0.24400−0.30000	231	-3.000 ± 0.944	-1.637	1.444	2.799	0.516	Accept H_0	-2.340
	5	0.30000−0.38300	231	-2.331 ± 0.615	-2.340	0.015	2.799	0.005	Accept H_0	-2.340
	6	0.38300−0.47800	231	-4.168 ± 0.544	-2.340	3.360	2.799	1.200	Reject H_0	-4.535
3.6μm	1	-0.07500−0.11000	270	-3.374 ± 0.355	—	—	—	—	—	—
	2	0.11000−0.16300	270	-4.051 ± 0.744	-3.374	0.909	2.795	0.325	Accept H_0	-3.594
	3	0.16300−0.21000	265	-4.005 ± 0.769	-3.594	0.535	2.796	0.191	Accept H_0	-3.673
	4	0.21000−0.26400	272	-2.995 ± 0.729	-3.673	0.929	2.795	0.333	Accept H_0	-3.448
	5	0.26400−0.33000	272	-3.418 ± 0.556	-3.448	0.054	2.795	0.019	Accept H_0	-3.447
	6	0.33000−0.44200	270	-4.106 ± 0.351	-3.447	1.876	2.795	0.671	Accept H_0	-3.889
	7	0.44200−0.55400	270	-2.640 ± 0.320	-3.889	3.909	2.795	1.398	Reject H_0	-2.143
4.5μm	1	-0.08100−0.11000	267	-2.933 ± 0.355	—	—	—	—	—	—
	2	0.11000−0.16300	269	-4.054 ± 0.796	-2.933	1.408	2.795	0.504	Accept H_0	-3.497
	3	0.16300−0.21000	269	-3.554 ± 0.865	-3.497	0.066	2.795	0.024	Accept H_0	-3.499
	4	0.21000−0.26400	272	-2.974 ± 0.774	-3.499	0.678	2.795	0.243	Accept H_0	-3.371
	5	0.26400−0.33000	271	-3.950 ± 0.607	-3.371	0.954	2.795	0.341	Accept H_0	-3.569
	6	0.33000−0.44200	270	-4.028 ± 0.369	-3.569	1.247	2.795	0.446	Accept H_0	-3.774
	7	0.44200−0.55400	272	-2.797 ± 0.340	-3.774	2.878	2.795	1.029	Reject H_0	-2.768
$W_{V,I}$	1	0.00500−0.11300	270	-3.933 ± 0.328	—	—	—	—	—	—
	2	0.11300−0.16500	266	-3.826 ± 0.586	-3.933	0.182	2.796	0.065	Accept H_0	-3.926
	3	0.16500−0.21100	273	-3.792 ± 0.600	-3.926	0.223	2.795	0.080	Accept H_0	-3.915
	4	0.21100−0.26300	269	-3.557 ± 0.503	-3.915	0.711	2.795	0.254	Accept H_0	-3.824
	5	0.26300−0.32600	272	-4.072 ± 0.423	-3.824	0.586	2.795	0.210	Accept H_0	-3.876
	6	0.32600−0.43800	270	-3.939 ± 0.273	-3.876	0.231	2.795	0.082	Accept H_0	-3.881
	7	0.43800−0.54500	269	-2.892 ± 0.302	-3.881	3.274	2.795	1.171	Reject H_0	-2.723
$V-I$	1	0.00500−0.11100	269	0.116 ± 0.119	—	—	—	—	—	—
	2	0.11100−0.16200	271	0.379 ± 0.234	0.116	1.126	2.795	0.403	Accept H_0	0.222
	3	0.16200−0.20700	267	-0.051 ± 0.261	0.222	1.044	2.796	0.374	Accept H_0	0.120
	4	0.20700−0.25800	273	0.440 ± 0.271	0.120	1.180	2.795	0.422	Accept H_0	0.255
	5	0.25800−0.32100	269	-0.078 ± 0.210	0.255	1.588	2.795	0.568	Accept H_0	0.066
	6	0.32100−0.42500	271	-0.276 ± 0.131	0.066	2.600	2.795	0.930	Accept H_0	-0.252
	7	0.42500−0.53800	270	0.375 ± 0.116	-0.252	5.398	2.795	1.931	Reject H_0	0.958

fore, any evidence of non-linearity is not influenced by the incompleteness bias. We also use our test statistics to determine the significance of the break at 2.95 days as observed in Subramanian & Subramaniam (2015). Both F-test and Random Walk imply a significant change in the slope of the multi-band PL relations at this period as well. Interestingly, the testimator also finds a change in the slope of optical band PL and Wesenheit relations in the period bin containing 2.95 days.

The plots of optical band PC relations for FU and FO mode Cepheids are shown in Fig. 10. The results of the test statistics are provided in Table 6 & 9 for F and random walk

Table 11. Summary of the matched OGLE-III LMC FO mode Cepheids with SAGE archival data. The meaning of each column header is discussed in Table 1.

Band	epoch	$N_{\rm match}$	$<\Delta>^a$	σ^b	^{c}(in %)
3.6μm	1	371	0.223	0.225	97.84
	2	818	0.129	0.171	99.02
4.5μm	1	364	0.220	0.214	98.08
	2	810	0.128	0.171	99.14
5.8μm	1	204	0.208	0.208	98.04
	2	464	0.126	0.178	99.14
8.0μm	1	69	0.278	0.329	94.20
	2	176	0.137	0.237	97.73

Table 12. Optical and mid-infrared band PL relations for LMC FO mode Cepheids.

Band	PL Slope	PL ZP	σ	N
V	-3.299 $\pm$ 0.029	16.865 $\pm$ 0.010	0.182	1084
I	-3.354 $\pm$ 0.021	16.294 $\pm$ 0.007	0.129	1084
$W_{V,I}$	-3.466 $\pm$ 0.011	15.415 $\pm$ 0.004	0.069	1075
3.6μm	-3.445 $\pm$ 0.017	15.490 $\pm$ 0.006	0.099	1055
4.5μm	-3.424 $\pm$ 0.018	15.460 $\pm$ 0.007	0.104	1049

test and in Table 7 & 10 for the testimator. All test statistics provide evidence of a significant change in the slope of PC relations for both FU and FO mode Cepheids having periods smaller/greater than 2.5 days. We have shown that the SMC FO mode PL relations do not provide evidence of a break at 1 day as suggested by Subramanian & Subramaniam (2015), if we restrict the sample size to $P < 2.5$ days. However, we do find a significant change in the slope of PC relation at 1 day for this case as well. There is also a significant deviation in the slope of PC at 2.95 days for FU mode Cepheids.

5 COMPARISON WITH LMC PL RELATIONS

We also compare our PL relations for SMC FO mode Cepheids with PL relations for LMC FO mode Cepheids. At optical wavelengths, the OGLE-III catalog has classified 1238 FO mode Cepheids in the LMC. We note that Bhardwaj et al. (2016) provided variation in the slope of PL relations for FO mode Cepheids in the LMC and tested for possible non-linearity. Therefore, we derive PL and PW relations for these FO mode Cepheids with similar period cut and sigma clipping as carried out for the FO mode Cepheids in the SMC, for relative comparison. Recently, Macri et al. (2015) derived new near-infrared PL relations for the LMC FO mode Cepheids based on time series observations. Therefore, we do not use 2MASS data to derive JHK_s PL relations as Macri et al. (2015) results are clearly superior in all aspects. These PL relations at $VIJHK_s$ wavelengths are tested to determine possible non-linearities in multiple wavelengths (Bhardwaj et al. 2016). We note that a detailed study on mid-infrared PL relations does not exist in literature for FO mode Cepheids. Therefore, we derive new LMC FO Cepheid PL relations at mid-infrared wavelengths for OGLE-III Cepheids.

We cross-matched OGLE-III LMC FO mode Cepheids with publicly released SAGE data using a search radius of 2″ and obtained IRAC band photometry for epoch 1 and 2. The number of matched sources and the corresponding mean separations and standard deviations are summarized in Table 11 for the SAGE data. We estimated the error weighted mean in case the magnitudes were available for more than one epoch of observation for a particular Cepheid. Similar to SMC FO mode Cepheids, the magnitudes in 5.8μm and 8.0μm-bands for LMC FO mode Cepheids are mostly affected by the incompleteness bias at short period ends and therefore, we do not consider these bands in deriving PL relations. We only make use of magnitudes in 3.6μm and 4.5μm-bands and correct them for extinction using the Haschke maps (Haschke, Grebel & Duffau 2011) as discussed previously. We restrict our sample for $P > 0.6$ days because there are very few stars below this period and apply recursive 2.5σ clipping before fitting PL relations.

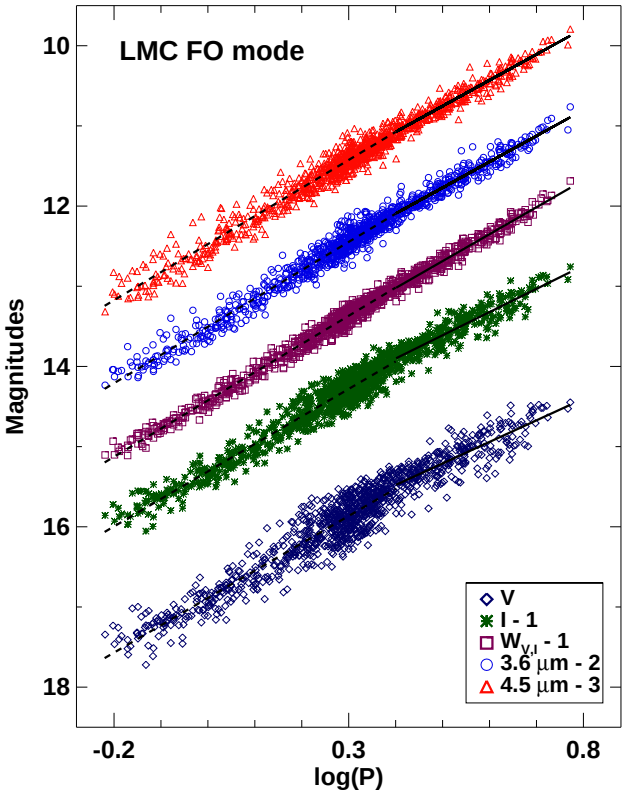

Figure 11. Multi band PL relations and Wesenheit function for LMC FO mode Cepheids. The solid/dashed lines represent the best fit regression for Cepheids with periods below and above 2.5 days.

Fig. 11 displays the PL relations for LMC FO mode Cepheids at optical and mid-infrared wavelengths and the optical Wesenheit relation while the results are presented in Table 12. We note that the dispersion in these PL relations is significantly smaller than those for the SMC FO mode PL relations. As suggested previously, the increased dispersion for the SMC FO mode PL relations may be attributed to the high line-of-sight depth of the galaxy (Subramanian & Subramaniam 2015). We note that Bhardwaj et al. (2016) found a significant break in optical

Table 13. Results of F and random walk tests for PL and PW relations for FO mode Cepheids in the LMC to test non-linearity at 2.5 days. The meaning of each column header is discussed in Table 6.

Y	PL Slope$_S$	PL ZP$_S$	σ_S	N_S	PL Slope$_L$	PL ZP$_L$	σ_S	N_S	F	$p(F)$	$p(R)$
For all P with a break at 2.5 days (Bhardwaj et al. 2014)											
V	-3.410±0.045	16.888±0.012	0.187	802	-2.688±0.108	16.554±0.057	0.155	282	16.080	0.000	0.000
I	-3.430±0.032	16.310±0.008	0.132	802	-2.894±0.078	16.058±0.041	0.112	282	17.231	0.000	0.000
3.6μm	-3.524±0.027	15.504±0.007	0.104	769	-3.231±0.057	15.386±0.030	0.079	286	11.088	0.000	0.000
4.5μm	-3.499±0.030	15.474±0.008	0.112	764	-3.223±0.055	15.364±0.029	0.077	285	8.845	0.000	0.001
$W_{V,I}$	-3.517±0.017	15.424±0.005	0.070	790	-3.359±0.045	15.366±0.024	0.066	285	9.145	0.000	0.000

Table 14. Results of the testimator on PL and PW relations for FO mode Cepheids in the LMC. The meaning of each column header is discussed in Table 7.

Band	n	log(P)	N	$\hat{\beta}$	β_0	$\lvert t_{obs}\rvert$	t_c	k	Decision	β_w
V	1	-0.21900−0.12700	180	-2.997±0.133	—	—	—	—	—	—
	2	0.12700−0.26400	172	-4.392±0.419	-2.997	3.329	2.669	1.247	Reject H_0	-4.737
I	1	-0.21900−0.12700	180	-3.045±0.101	—	—	—	—	—	—
	2	0.12700−0.26500	179	-3.707±0.284	-3.045	2.328	2.668	0.872	Accept H_0	-3.623
	3	0.26500−0.31000	179	-3.138±0.790	-3.623	0.613	2.668	0.230	Accept H_0	-3.511
	4	0.31000−0.36400	181	-3.467±0.607	-3.511	0.074	2.668	0.028	Accept H_0	-3.510
	5	0.36400−0.47000	181	-3.386±0.257	-3.510	0.482	2.668	0.181	Accept H_0	-3.488
	6	0.47000−0.77200	183	-2.887±0.133	-3.488	4.532	2.667	1.699	Reject H_0	-2.466
3.6μm	1	-0.21900−0.14100	170	-3.251±0.099	—	—	—	—	—	—
	2	0.14100−0.26700	168	-3.434±0.229	-3.251	0.799	2.670	0.299	Accept H_0	-3.306
	3	0.26700−0.31000	172	-4.158±0.717	-3.306	1.189	2.669	0.445	Accept H_0	-3.685
	4	0.31000−0.36000	169	-3.484±0.527	-3.685	0.381	2.670	0.143	Accept H_0	-3.657
	5	0.36000−0.45300	171	-3.376±0.217	-3.657	1.291	2.669	0.483	Accept H_0	-3.521
	6	0.45300−0.77200	204	-3.195±0.082	-3.521	3.962	2.664	1.487	Reject H_0	-3.036
4.5μm	1	-0.21900−0.14300	170	-3.317±0.119	—	—	—	—	—	—
	2	0.14300−0.26800	169	-3.560±0.252	-3.317	0.961	2.670	0.360	Accept H_0	-3.405
	3	0.26800−0.31000	169	-4.685±0.737	-3.405	1.738	2.670	0.651	Accept H_0	-4.238
	4	0.31000−0.36200	172	-3.484±0.480	-4.238	1.572	2.669	0.589	Accept H_0	-3.794
	5	0.36200−0.45700	167	-3.595±0.240	-3.794	0.829	2.670	0.310	Accept H_0	-3.732
	6	0.45700−0.77200	201	-3.177±0.080	-3.732	6.908	2.665	2.592	Reject H_0	-2.294
$W_{V,I}$	1	-0.21900−0.12800	170	-3.302±0.059	—	—	—	—	—	—
	2	0.12800−0.26400	165	-3.535±0.161	-3.302	1.452	2.670	0.544	Accept H_0	-3.428
	3	0.26400−0.30600	174	-3.795±0.483	-3.428	0.759	2.669	0.284	Accept H_0	-3.533
	4	0.30600−0.35300	169	-3.483±0.352	-3.533	0.140	2.670	0.052	Accept H_0	-3.530
	5	0.35300−0.44000	170	-3.357±0.172	-3.530	1.007	2.669	0.377	Accept H_0	-3.465
	6	0.44000−0.77200	226	-3.383±0.058	-3.465	1.406	2.662	0.528	Accept H_0	-3.422

band relations at $\log P = 0.4$ for LMC FO mode Cepheids but no such break is observed in near-infrared PL relations. We also test for possible non-linearity in PL relations derived in this study for FO mode Cepheids at 2.5 days. The results of the F-test, random walk and the testimator are presented in Table 13 and 14. The optical band PL relations provide significant change in slope around 2.5 days, similar to SMC FO mode Cepheids. Interestingly, the mid-infrared PL relations also provide evidence of a significant break at $\log P = 0.4$. The F and random walk test suggest the probabilities of acceptance of null hypothesis i.e. a linear relation, are approximately zero. Therefore, a significant change is observed in the slope of the PL relations at 2.5 days for LMC FO mode Cepheids at 3.6 & 4.5μm wavelengths.

We provide a detailed comparison of the slopes for FO mode Cepheid PL relations between the LMC and SMC in the period range $0.6 < P < 6.3$ days and the results are presented in Table 15. The t-test suggests that the optical V-band and the Wesenheit function are not consistent in the two clouds, while the I-band PL relations exhibit similar slopes with a marginal difference. Most of these relations in the infrared are consistent, given the uncertainties in the slopes, except in the case of the J and 3.6μm band PL relations. The difference in the slopes for the two clouds is least in I-band and 4.5μm-band PL relations.

5.1 Distance modulus between the SMC and LMC using FO mode Cepheids

We determine the relative distance modulus between the SMC and LMC based on multiband P-L relations for FO mode Cepheids. We fit an equation to each band PL relations in the Magellanic Clouds in the following form :

Table 15. Comparison of the slopes of FO mode Cepheid PL relations between the SMC and LMC.

Band	Galaxy	PL Slope	σ	N	$\lvert\Delta\rvert^a \pm \sigma^b_\Delta$	Src	$\lvert T\rvert$	$p(t)$
V	SMC	-3.147±0.035	0.268	1531	0.152±0.045	TW	3.124	0.002
	LMC	-3.299±0.029	0.182	1084		B15	—	—
I	SMC	-3.332±0.028	0.218	1531	0.022±0.035	TW	0.569	0.569
	LMC	-3.354±0.021	0.129	1084		B15	—	—
J	SMC	-3.095±0.055	0.198	595	0.202±0.059	TW	3.859	0.000
	LMC	-3.297±0.020	0.134	475		M15	—	—
H	SMC	-3.151±0.053	0.191	598	0.064±0.057	TW	1.319	0.187
	LMC	-3.215±0.020	0.100	475		M15	—	—
K_s	SMC	-3.132±0.083	0.197	457	0.113±0.086	TW	1.579	0.115
	LMC	-3.245±0.023	0.086	475		M15	—	—
3.6μm	SMC	-3.510±0.024	0.180	1499	0.065±0.029	TW	1.969	0.049
	LMC	-3.445±0.017	0.099	1055		TW	—	—
4.5μm	SMC	-3.451±0.028	0.200	1529	0.027±0.033	TW	0.723	0.470
	LMC	-3.424±0.018	0.104	1049		TW	—	—
$W_{V,I}$	SMC	-3.626±0.020	0.153	1526	0.160±0.023	TW	6.193	0.000
	LMC	-3.466±0.011	0.069	1075		B15	—	—

Notes: Source: TW - this work; M15 - Macri et al. (2015); B15 - Bhardwaj et al. (2016). $^a\Delta$ is the difference in the slopes of LMC and SMC PL relations. The error (σ^b_Δ) is obtained using the quadrature sum of the errors in two slopes.

Table 16. Distance modulus between LMC and SMC estimated using FO mode Cepheids.

Band	a_S	a_L	$\mu_{SMC} - \mu_{LMC}$
V	-3.301±0.030	-2.782±0.093	0.422±0.013
I	-3.418±0.023	-2.962±0.073	0.462±0.010
J	-3.239±0.059	-2.990±0.097	0.448±0.018
H	-3.204±0.050	-3.121±0.090	0.532±0.015
K_s	-3.303±0.062	-3.099±0.077	0.495±0.014
3.6μm	-3.534±0.022	-3.177±0.054	0.513±0.009
4.5μm	-3.494±0.026	-3.178±0.057	0.497±0.010
$W_{V,I}$	-3.621±0.016	-3.266±0.050	0.519±0.007
			$\Delta\mu = 0.49 \pm 0.02$

Note : The last column represents the relative distance modulus. a is the slope and subscripts S and L represent short ($P < 2.5$ days) and long ($P > 2.5$ days) period range Cepheids.

$$m = (\mu_{SMC} - \mu_{LMC}) + b_{LMC} + a_S \log P_S + a_L \log P_L, \quad (1)$$

where, m is the magnitude for Cepheids in the Magellanic Clouds in a particular band. The first term, $(\mu_{SMC}-\mu_{LMC})$, provides the relative distance modulus between the Magellanic Clouds. The coefficients, a and b represent the slope and intercept, respectively and the subscript S and L represent the short (P<2.5 days) and long (P>2.5 days) period Cepheids. We use two slope linear regression in our analysis as optical band PL relations provide evidence of statistically significant non-linearities at 2.5 days.

We provide the slopes and relative distance moduli between SMC and LMC in Table 16. We note that the difference in the relative distance modulus varies significantly from optical to infrared bands. We estimate the mean and standard deviation of all relative distances and adopt an average relative distance modulus of $\Delta\mu = 0.49 \pm 0.02$. This value is consistent with those based on FU mode Cepheids (0.48 ± 0.02) derived by Ngeow et al. (2015). We also note that de Grijs, Wicker & Bono (2014) and de Grijs & Bono (2015) recommended a distance modulus of 18.49±0.09 mag and 18.96 ± 0.02 mag for LMC and SMC, respectively. The relative distance modulus between the two clouds based on these recommended distances is 0.47 ± 0.09 mag. Therefore, our estimated relative distance modulus is in good agreement with the difference in recommended distance moduli of the two Clouds.

6 CONCLUSIONS

In this work, we derive new multi-band PL relations for first-overtone mode Cepheids in the SMC. In addition to a large compilation of OGLE-III Cepheids, we use their counterparts in 2MASS and SAGE catalogs to derive multi-band mean magnitudes for Cepheids in the SMC. The extinction corrections are done using the Haschke maps (Haschke, Grebel & Duffau 2011). We also extend the work of Ngeow et al. (2015) to include short period SMC fundamental-mode Cepheids in our analysis. We use robust statistical tests such as, F-test, random walk test and the testimator, to determine the significance of possible non-linearities at various periods in PL relations for fundamental and first-overtone mode Cepheids in the SMC. We also derive new optical and mid-infrared band PL relations for first-overtone mode Cepheids in the LMC. The first-overtone mode PL relation in the Magellanic Clouds are compared and we find that most of these relations are not consistent in the two clouds. We summarize the main results from our study as follows.

- The multi-band PL relations for FO mode Cepheids in the Magellanic Clouds, derived in this study, are found to be consistent with previous studies in the literature. The updated infrared band PL relations for FO mode Cepheids are not studied in detail previously, and will be highly relevant in the upcoming era of the *James Webb Space Telescope*.

• We find significant evidence of a break in PL relations for both fundamental and first-overtone mode Cepheids in the SMC at 2.5 days at optical bands. The fundamental-mode SMC Cepheids also exhibit this break in infrared band PL relations. We do not find any evidence of non-linearity at 1 days as observed by Subramanian & Subramaniam (2015) for first-overtone mode SMC Cepheids.

• Our analysis suggests that these breaks are related to changes in the progression of light curve parameters with period for Classical Cepheids in the SMC. This is an important result in a sense that modelling these non-linearities in PL relations, i.e. physical parameters, together with changes in the Fourier parameters will be used to constrain theoretical pulsation codes and determine mass-luminosity relations obeyed by Cepheids in the Magellanic Clouds.

• We also compare the multi-band PL relations in the Magellanic clouds for first-overtone mode Cepheids. The slope of the PL relations in the two clouds are not consistent at optical bands, presumably due to significant non-linearities. We estimate the relative distance modulus of $\Delta\mu = 0.49 \pm 0.02$ mag, between the two clouds using multi-band PL relations for first-overtone mode Cepheids in the SMC and LMC.

• The various non-linearities and the inconsistency in the slopes between the two clouds may be related to the metallicity differences thus leading to different Cepheid mass-luminosity relations. Bhardwaj et al. (2014) have provided a possible explanation for breaks in Period-Color relations at a period of 10 days based on the theory of hydrogen ionization front-stellar photosphere interaction as a function of pulsation phase. Further study will be required to discern the cause of nonlinearities at shorter periods. In future, with more infrared data coming from The VISTA near-infrared YJK_s survey of the Magellanic System (VMC) survey (Cioni et al. 2011; Ripepi et al. 2012, 2016), these relations will be studied as a function of pulsation phase to understand the metallicity dependence on the universality of Cepheid PL relations.

ACKNOWLEDGMENTS

We thank the anonymous referee for his/her valuable comments which improved the content and quality of the manuscript. AB is thankful to the Council of Scientific and Industrial Research, New Delhi, for the Senior Research Fellowship grant 09/045(1296)/2013-EMR-I. This work is supported by the grant for the Joint Center for Analysis of Variable Star Data provided by Indo-U.S. Science and Technology Forum. CCN thanks the funding from Ministry of Science and Technology (Taiwan) under the contract NSC101-2112-M-008-017-MY3 and NSC104-2112-M-008-012-MY3. HPS thanks University of Delhi for a R&D grant. This work also makes use of data products from the 2MASS survey, which is a joint project of the University of Massachusetts and the Infrared Processing and Analysis Center/California Institute of Technology, funded by the National Aeronautics and Space Administration and the National Science Foundation. In addition, this study also makes use of NASA's Astrophysics Data System, the VizieR catalogues.

REFERENCES

Bauer F. et al., 1999, AAP, 348, 175
Bhardwaj A., Kanbur S. M., Singh H. P., Ngeow C.-C., 2014, MNRAS, 445, 2655
Bhardwaj A., Kanbur S. M., Macri L. M., Singh H. P., Ngeow C.-C., Wagner-Kaiser R., Sarajedini A., 2015a, Accepted in AJ, ArXiv e-prints, 1510.03682
Bhardwaj A., Kanbur S. M., Singh H. P., Macri L. M., Ngeow C.-C., 2015b, MNRAS, 447, 3342
Bhardwaj A., Kanbur S. M., Macri L. M., Singh H. P., Ngeow C.-C., Ishida E. E. O., 2016, MNRAS, 457, 1644
Bono G., Groenewegen M. A. T., Marconi M., Caputo F., 2002, ApJL, 574, L33
Caldwell J. A. R., Laney C. D., 1991, in IAU Symposium, Vol. 148, The Magellanic Clouds, Haynes R., Milne D., eds., p. 249
Cardelli J. A., Clayton G. C., Mathis J. S., 1989, APJ, 345, 245
Cioni M.-R. L. et al., 2011, A&A, 527, A116
Cutri R. M. et al., 2003, VizieR Online Data Catalog, 2246, 0
de Grijs R., Wicker J. E., Bono G., 2014, AJ, 147, 122
de Grijs R., Bono G., 2015, AJ, 149, 179
Deb S., Singh H. P., 2009, A&A, 507, 1729
Groenewegen M. A. T., 2000, A&A, 363, 901
Haschke R., Grebel E. K., Duffau S., 2011, AJ, 141, 158
Inno L. et al., 2013, ApJ, 764, 84
Inno L. et al., 2015, A&A, 576, A30
Planck collaboration, Ade P. A. R. et al., 2014, A&A, 571, A16
Laney C. D., Stobie R. S., 1986, MNRAS, 222, 449
Laney C. D., Stobie R. S., 1994, MNRAS, 266, 441
Leavitt H. S., Pickering E. C., 1912, Harvard College Observatory Circular, 173, 1
Macri L. M., Ngeow C.-C., Kanbur S. M., Mahzooni S., Smitka M. T., 2015, AJ, 149, 117
Matsunaga N., Feast M. W., Soszyński I., 2011, MNRAS, 413, 223
Ngeow C.-C., Kanbur S. M., 2010, ApJ, 720, 626
Ngeow C.-C., Citro D. M., Kanbur S. M., 2012, MNRAS, 420, 585
Ngeow C.-C., Kanbur S. M., Bhardwaj A., Singh H. P., 2015, ApJ, 808, 67
Riess A. G. et al., 2009, ApJ, 699, 539
Riess A. G. et al., 2011, ApJ, 730, 119
Ripepi V. et al., 2012, MNRAS, 424, 1807
Ripepi V. et al., 2016, arXiv:1602.09005
Sandage A., 1988, PASP, 100, 935
Sandage A., Tammann G. A., Reindl B., 2009, A&A, 493, 471
Sharpee B., Stark M., Pritzl B., Smith H., Silbermann N., Wilhelm R., Walker A., 2002, AJ, 123, 3216
Soszyński I., Gieren W., Pietrzyński G., 2005, PASP, 117, 823
Soszyñski I. et al., 2010, Acta Astron., 60, 17
Storm J., Carney B. W., Gieren W. P., Fouqué P., Latham D. W., Fry A. M., 2004, A&A, 415, 531
Subramanian S., Subramaniam A., 2015, A&A, 573, A135
Tammann G. A., Sandage A., Reindl B., 2003, A&A, 404, 423
Tammann G. A., Reindl B., Sandage A., 2011, A&A, 531,

A134
Udalski A., Soszynski I., Szymanski M., Kubiak M., Pietrzynski G., Wozniak P., Zebrun K., 1999a, Acta Astron., 49, 437
Udalski A., Szymanski M., Kubiak M., Pietrzynski G., Soszynski I., Wozniak P., Zebrun K., 1999b, Acta Astron., 49, 201
Welch D. L., Madore B. F., 1984, in IAU Symposium, Vol. 108, Structure and Evolution of the Magellanic Clouds, van den Bergh S., de Boer K. S. D., eds., p. 221
Welch D. L., McLaren R. A., Madore B. F., McAlary C. W., 1987, ApJ, 321, 162